Int. J. Heat Mass Transfer. Vol. 22, pp. 929 939
© Pergamon Press Ltd. 1979. Printed in Great Britain

0017-9310/79/0601-0929 $02.00/0

NATURAL CONVECTION IN POROUS MEDIA BOUNDED BY CONCENTRIC SPHERES AND HORIZONTAL CYLINDERS

P. J. BURNS† and C. L. TIEN‡

(*Received* 28 *June* 1978 *and in revised form* 27 *November* 1978)

Abstract—The present paper reports the results of an analytical investigation of natural convection in porous media completely enclosed by concentric spheres and horizontal cylinders. The steady, two-dimensional problem has been solved by the method of finite differences and the method of regular perturbations. The variations of the overall heat transfer with the modified Rayleigh number, the non-dimensional external heat-transfer coefficient, and the radius ratio have been assessed. Results indicate that a maximum value of the heat transfer occurs for the spherical and cylindrical geometries dependent solely upon the radius ratio for each geometry. The flow field has been examined and compared for the two geometries. An interesting feature is manifested by the occurrence of a relatively stagnant and stable cold region at the bottom of the enclosure if the inner bounding surface is considered to be heated, thus shifting the center of the gross circulation from the horizontal. Additionally, a possible qualitative analogy between the nature of the free convection when the enclosure is filled with a porous medium and when the enclosure is filled solely with a Newtonian fluid is scrutinized. Finally, some algebraic correlations of the data are set forth for the convenience of practical applications.

NOMENCLATURE

Bi, Biot number, $h(\Delta R)/k$;
c_p, specific heat of the fluid [J/kg K];
Da, Darcy number, $K/(\Delta R)^2$;
$\mathbf{e}$, position vector;
$f(\eta), g(\eta)$, function in the perturbation analysis indicative of the dependence of the heat transfer upon the radius ratio, cylindrical geometry and spherical geometry, respectively;
g, acceleration of gravity [m/s^2];
h, heat-transfer coefficient [W/m^2 K];
K, permeability [m^2];
k, thermal conductivity of the stagnant porous medium [W/m K];
k_{eff}, effective thermal conductivity including the effects of convection and radiation [W/m K];
M, N, number of grid spaces in the radial and azimuthal directions, respectively;
Nu, Nusselt number defined by equation (10);
$\bar{p}$, pressure [N/m^2];
R_j, radial coordinate at a boundary [m];
r, non-dimensional radial position;
$\bar{r}$, radial coordinate [m];
ΔR, radial distance between inner and outer boundaries [m];
Ra, modified Rayleigh number, $g\beta(\Delta T)K(\Delta R)/\nu\alpha$;
Ra^*, modified Rayleigh number, perturbation solution, $g\beta(\Delta T)KR_0/\nu\alpha$;
$\overline{Ra}$, Rayleigh number, $g\beta(\Delta T)K(\Delta R)^3/\nu\alpha_0$;
T, temperature [K];
ΔT, temperature difference between the internal boundary and the external environment, $T_i - T_0$ [K];
$\bar{u}$, radial velocity [m/s];
$\bar{\mathbf{V}}$, vectorial velocity, $\bar{u}\mathbf{e}_1 + \bar{v}\mathbf{e}_2 + \bar{w}\mathbf{e}_3$ [m/s];
$\bar{v}$, azimuthal velocity [m/s];
$\bar{w}$, polar or longitudinal velocity [m/s];
X, denotes position of the maximum negative value of the stream function.

Greek symbols

α, thermal diffusivity of the stagnant porous medium, $k/\rho c_p$ [m^2/s];
α_0, thermal diffusivity, $k_0/\rho c_p$ [m^2/s];
β, coefficient of cubical expansion $(1/K)$;
η, radius ratio, R_i/R_0;
θ, non-dimensional temperature, $(T - T_0)/(T_i - T_0)$;
μ, absolute viscosity [N s/m^2];
ν, kinematic viscosity [m^2/s];
ρ, density of the fluid [kg/m^3];
ϕ, azimuthal angle;
ψ, non-dimensional stream function defined by equation (8).

Subscripts

i, pertaining to the inside boundary or a defining quantity;
j, general subscriptive variable;
0, pertaining to the external environment or the outside boundary, or pertaining to the Newtonian fluid;
r, pertaining to the radial direction;
s, pertaining to the interior porous medium;
ϕ, pertaining to the azimuthal direction;
∞, pertaining to the exterior environment.

†Assistant Professor of Mechanical Engineering, Colorado State University, Fort Collins, CO 80523, U.S.A.
‡Professor of Mechanical Engineering, University of California, Berkeley, CA 94720, U.S.A.

INTRODUCTION

BECAUSE of their minimum surface area-to-volume ratio, spherical storage tanks will be established due to increasing energy conservation measures. The question as to the nature of the most effective procedure of insulating these facilities from heat loss naturally arises. Many of the existing available "superinsulations" necessitate considerable expense in capital investment, and the maintenance of moderately high vacuums to reduce heat loss [1] incurs additional expense. Simple thermos-bottle type systems are one alternative, but relatively large structural supports with an associated reduction in overall insulating capacity are usually necessary to provide the requisite strength in massive systems. Other practical problems also exist in the use of such systems.

A variety of such superinsulations have been analyzed, yet little attention has been afforded to the insulating characteristics of porous materials in non-rectangular geometries. A fundamental investigation of the thermal performance of such insulations would produce results aiding the practicing engineer in attaining a judicious design decision.

A porous material is introduced into an enclosure to decrease the convective and radiative transfer of heat. Although radiation may significantly contribute to the total heat transfer at elevated temperatures, around room temperature the effect is small [2–4] and is lumped into the experimentally determined thermal conductivity. Thus, the transport of heat by radiation and convective motion is reduced at the expense of an increased amount of heat transfer by conduction. The correspondingly complicated flow system is described in a macroscopic sense by Darcy's law [5–7].

Many published works have dealt with free convection in porous media heated from below. An excellent current review was presented by Bankvall [8]. The conjugate problem of heating from the side has yet to be as thoroughly examined. Experimental [8–13] and theoretical [8, 9, 11, 12, 14, 15] results are available for a variety of rectangular configurations and insulation materials. Existing studies concerning the cylindrical geometry are few in number, while studies concerning the spherical geometry are non-existent.

Caltagirone has presented an extensive treatment of free convection in a porous medium ensconced between horizontal concentric cylinders [16]. The evolution of various flow patterns was established as the temperature difference was increased. Two-dimensional, steady solutions were obtained numerically and utilizing a perturbation technique. Experimental verification was sought, and unsteady and three-dimensional patterns were observed. Critical Rayleigh numbers were established from a solution employing the Galerkin technique, and some unsteady, three-dimensional flows were generated numerically utilizing the method of finite elements. Although specific heat-transfer data were presented, the subject was not treated in general as the author's main emphasis was upon the nature of the fluid flow. Two-dimensional results for the average and local heat-transfer rates have also been presented by Brailovskaya *et al.* [17].

ANALYTICAL FORMULATION

The porous medium is assumed to be an effective continuum. This is generally valid for systems where the non-dimensional pore space, the square of which is qualitatively represented by the Darcy number, $K/(\Delta R)^2$, is much less than one. Darcy's law then adequately describes the transfer of momentum provided the Reynolds number based upon pore diameter is less than one [6, 7, 18] so that inertial effects are yet negligible. The Boussinesq approximation of constant properties except in the body force term is utilized, limiting the overall temperature difference. The continuity equation and the equations governing the transfer of momentum and energy in the steady state are, in dimensional form, as follows [7]:

$$\nabla \cdot \bar{\mathbf{V}} = 0 \tag{1}$$

$$\bar{\mathbf{V}} = \frac{-K}{\mu}[\nabla \bar{p} - \rho \mathbf{g}] \tag{2}$$

$$\bar{\mathbf{V}} \cdot \nabla T = \alpha \nabla^2 T. \tag{3}$$

The physical system is shown in Fig. 1. The azimuthal angle is measured counterclockwise from the vertically down position. The gravity vector is represented by:

$$\mathbf{g} = g[\cos\phi \mathbf{e}_r - \sin\phi \mathbf{e}_\phi]. \tag{4}$$

The inner sphere or cylinder is of radius R_i and the outer of radius R_0. The most representative distance with which to non-dimensionalize the physical variables is taken as the gap thickness, $\Delta R = R_0 - R_i$.

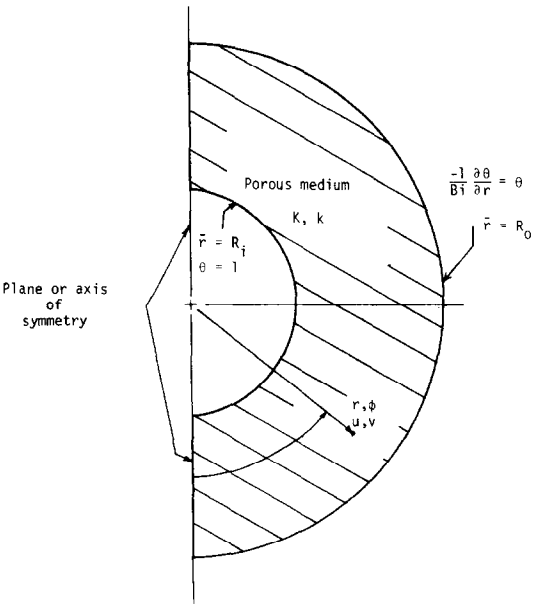

FIG. 1. The physical system.

The annular space between the concentric spheres or cylinders is filled with a porous medium of permeability K, and stagnant thermal conductivity k_0.

The variables $\bar{r}$, ϕ, $\bar{u}$, $\bar{p}$ and T are non-dimensionalized as follows:

$$\frac{\bar{r}}{\Delta R}, \phi, \frac{\bar{u}(\Delta R)}{\alpha}, \frac{\bar{p}K}{\mu\alpha}, \frac{T-T_0}{T_i-T_0} \tag{5}$$

to yield the unbarred quantities, r, ϕ, u, p and θ, respectively.

The curl of equation (2) is taken to eliminate the pressure, and a non-dimensional stream function is defined to satisfy the continuity equation. The resulting system of non-dimensional equations expanded for the spherical geometry are as follows:

$$r^2\frac{\partial^2\psi}{\partial r^2} + \sin\phi\frac{\partial}{\partial\phi}\left(\frac{1}{\sin\phi}\frac{\partial\psi}{\partial\phi}\right) = -Rar^2\sin\phi\left[r\frac{\partial\theta}{\partial r}\sin\phi + \frac{\partial\theta}{\partial\phi}\cos\phi\right] \tag{6}$$

$$\frac{\partial\psi}{\partial\phi}\frac{\partial\theta}{\partial r} - \frac{\partial\psi}{\partial r}\frac{\partial\theta}{\partial\phi} = \sin\phi\frac{\partial}{\partial r}\left(r^2\frac{\partial\theta}{\partial r}\right) + \frac{\partial}{\partial\phi}\left(\sin\phi\frac{\partial\theta}{\partial\phi}\right) \tag{7}$$

$$u \equiv \frac{1}{r^2\sin\phi}\frac{\partial\psi}{\partial\phi}; \quad v \equiv \frac{-1}{r\sin\phi}\frac{\partial\psi}{\partial r}. \tag{8}$$

The non-dimensional parameter appearing in the coupling source term of equation (6) is the modified Rayleigh number, herein called the Rayleigh number for brevity. Explicitly:

$$Ra = \frac{g\beta(\Delta T)K(\Delta R)}{\nu\alpha}. \tag{9}$$

For ordinary porous insulation systems, the modified Rayleigh number is limited to less than about 100. Qualitatively, the modified Rayleigh number is the ratio of a buoyant force to the drag force of the medium, and increases as the imposed temperature difference is increased and the porosity or permeability is increased.

The total amount of heat necessary to maintain the steady state is characterized by the average Nusselt number, explicitly:

$$Nu = \frac{1}{A}\int\frac{\partial\theta}{\partial r}\mathrm{d}A\Big/\left(\frac{\partial\theta}{\partial r}\right)_{\mathrm{cond}} = \frac{k_{\mathrm{eff}}}{k} \tag{10}$$

where A is the area through which the heat is transferred and the subscript "cond" indicates that conduction is the only mode of heat transfer. With a lower bound of one, the average Nusselt number is the ratio of the total heat transfer to the heat transfer as if it occurred by conduction alone, or the ratio of the effective thermal conductivity to the thermal conductivity of the stagnant medium.

All boundaries are considered to be impermeable so that no normal velocity is allowed. Therefore:

$$\psi(r_i, r_0; \phi) = 0 \tag{11}$$

$$\psi(r; 0, \pi) = 0. \tag{12}$$

It is noted in passing the L'Hopital's rule must be utilized in evaluating u for the spherical system at $\phi = 0$ and π because the sine is zero at these locations.

The inner boundary is considered isothermal as would exist in storage tanks or pipes with walls of small thermal resistance compared to the insulation. The outer boundary is allowed to transfer heat with the surroundings at temperature, T_0, by virtue of a constant heat-transfer coefficient, h. If the heat-transfer coefficient becomes infinitely large, the outer boundary would become isothermal at temperature, T_0. The mathematical expressions for these boundary conditions are:

$$\frac{\partial\theta}{\partial r}(r; 0, \pi) = 0 \tag{13}$$

$$\theta(r_i, \phi) = 1 \tag{14}$$

$$-\frac{1}{Bi}\frac{\partial\theta}{\partial r}(r_0, \phi) = \theta(r_0, \phi) \tag{15}$$

where:

$$Bi = \frac{h(\Delta R)}{k}. \tag{16}$$

The problem may be parametrically stated as follows:

$$Nu = Nu(Ra, \eta, Bi) \tag{17}$$

where the second parameter, $\eta = R_i/R_0$, has been defined for convenience in the presentation of the results. In general, the average Nusselt number, hereafter called the Nusselt number, falls in the range of one to ten, and increases with increasing values of Ra and increasing values of Bi. The dependence on η, however, is somewhat complicated.

METHODS OF SOLUTION

The systems of equations and appropriate boundary conditions were solved using a regular perturbation approach which will be discussed subsequently and a finite-difference successive over-relaxation approach. The computation was accomplished by a CDC 7600 computer employing central-difference representations [19] of the governing equations and boundary conditions.

The calculation scheme proceeded as follows: (1) the stream function, ψ, and the temperature, θ, were initialized to their conduction values, i.e. variations with ϕ were neglected; (2) new stream function and temperature values were calculated from the central-difference forms of the governing equations; (3) new boundary temperature values were computed on the outer boundary, if necessary; (4) steps 2 and 3 were repeated until convergence was achieved; and (5) velocities and Nusselt numbers were computed from the converged fields.

The solutions were assumed to be converged to "steady-state" when the following criterion was satisfied:

$$\left|\frac{\tau_{\mathrm{new}} - \tau_{\mathrm{old}}}{\tau_{\mathrm{new}}}\right|_{\mathrm{max}} \leqslant \mathrm{Res} \tag{18}$$

where the subscript "max" denotes the maximum

value over all the grid points, and the symbol, τ, denotes any dependent variable, either the stream function or the temperature. The value of Res to achieve acceptable convergence was found to be 5×10^{-4}, as the value of the Nusselt number was found to change by less than 1% when Res was decreased from 5×10^{-4} to 5×10^{-5}.

A uniform grid system was employed in solving this problem (i.e. $\Delta r = 1/M$ and $\Delta\phi = \pi/N$). The accuracy of the scheme was determined by decreasing the grid size and observing the change in the quantities of the Nusselt number and the negative maximum of the stream function. The grid size was decreased until less than a 2% change was observed in these quantities for $Ra = 50$ and $\eta = 1/2$.

NUMERICAL RESULTS AND DISCUSSION

All calculations were performed for Rayleigh numbers of 10, 30, 50 and 75. The radius ratio was varied from 0.1 to 0.95 for isothermal boundaries and from 0.33 to 0.95 for a non-isothermal outer boundary. The Biot number was assigned values of ∞, 100, 50, 25, 12.5, 6.25 and 3.125. For air at room temperature and $(\Delta R) = 0.1$ m, this corresponds to values of about ∞, 25, 12, 6, 3, 2 and 1 [W/m^2 K] for the heat-transfer coefficient.

Figure 2 presents the variation of the Nusselt number, Nu, and the quantity $(-\psi)_{max} \times (1-\eta)$ indicative of the total mass circulating in the enclosure, with the radius ratio, η, for the spherical geometry. The influence of the free convective motion upon the Nusselt number is directly indicated by the value of the ordinate with the lower bound of one denoting pure conduction.

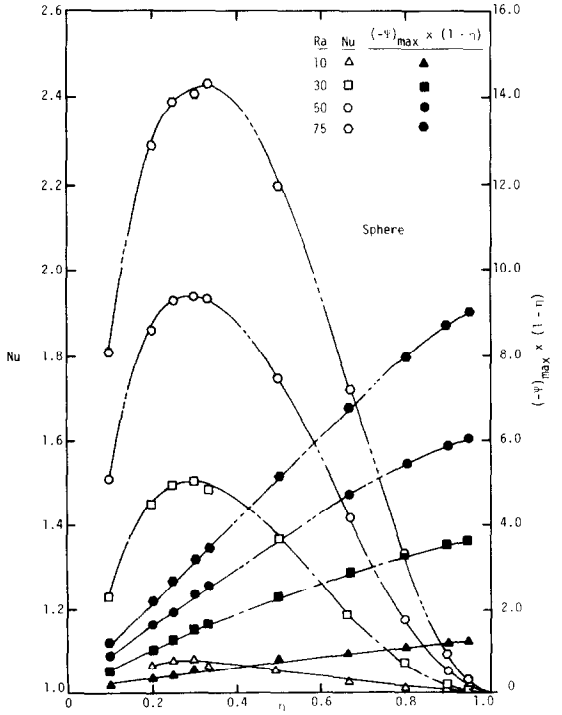

FIG. 2. The variation of the Nusselt number and the gross circulation with the radius ratio.

It is of interest to note that the curves possess a maximum value near a radius of 0.3. The small absolute value of the curvature and the degree of accuracy of the results do not permit a conclusive observation of a shift in the value of the abscissa at the maximum point as the Rayleigh number increases. Convection does not contribute to the Nusselt number as η approaches 1 because the ratio of the path length of the convective motion to the path length for conduction approaches infinity. As η is decreased from one, this ratio decreases resulting in an increased role of the free convective motion and a corresponding increase in the Nusselt number.

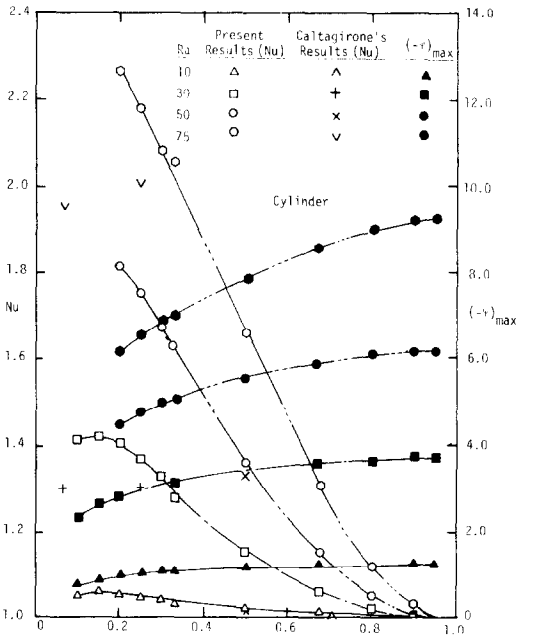

FIG. 3. The variation of the Nusselt number and the gross circulation with the radius ratio.

An opposing effect is the decrease in the amount of heat liberated as η is decreased since the relative size of the inner sphere is decreased. The effects balance around $\eta = 0.3$, and the Nusselt number is observed to decrease to 1 as η is further decreased to zero.

The variation of the Nusselt number and the negative maximum of the stream function (which is a measure of the gross circulation) with the radius ratio is shown in Fig. 3 for the cylindrical geometry. The physical situation is seen to be similar to the spherical geometry case. A maximum value of the Nusselt number occurs at $\eta = 0.15$. The maximum occurs "later" as η is decreased from 1 than occurs for the spherical geometry because the inner area decreases less rapidly for the cylindrical geometry. The results for the Nusselt number are compared with those of Caltagirone [16] where the values of the Rayleigh number are compatible. Agreement is fair except near $\eta = 0.15$ where the velocities are high and the grid spacing approaches the size of the inner cylinder.

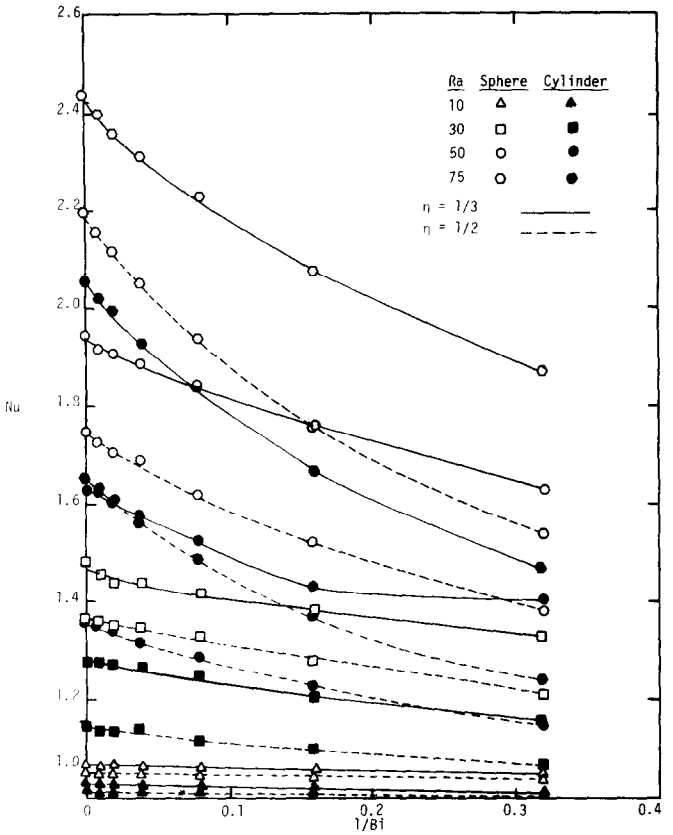

FIG. 4. The variation of the Nusselt number with the inverse of the Biot number for radius ratios of $\frac{1}{3}$ and $\frac{1}{2}$.

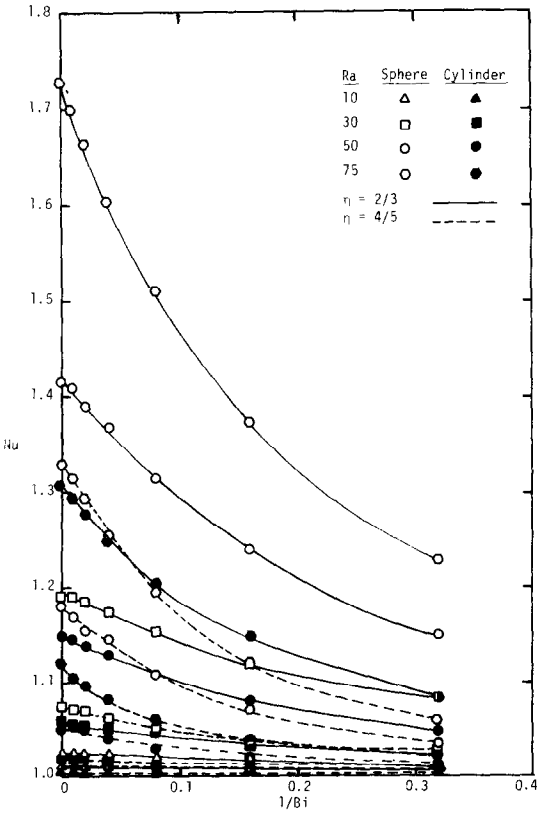

FIG. 5. The variation of the Nusselt number with the inverse of the Biot number for radius ratios of $\frac{2}{3}$ and $\frac{4}{5}$.

Figures 4–6 depict the variation of the Nusselt number with the inverse of the Biot number for both the spherical and cylindrical geometries for radius ratios of $\eta = 1/3$, 1/2 and 2/3, 4/5 and 9/10, respectively. The abscissa represents the ratio of the thermal resistance of the external medium to the thermal resistance of the effective porous medium on a Cartesian basis. The relations of the actual resistance ratios to be abscissas must include area variations.

The Nusselt number is seen to decrease as the inverse of the Biot number is increased. The outer boundary now assumes a local temperature between 0 and 1 according to the balance of radial heat fluxes at the surface. This acts to effectively decrease the average Rayleigh number for the enclosure by reducing the average temperature difference between the inside and outside boundaries. Since the local temperature on the outer boundary is proportional to the strength of the local free convective motion within, the most significant reductions in the heat transfer will occur at the higher rates of heat transfer. The variation of the Nusselt number with the inverse of the Biot number is thus seen to possess a large negative curvature at $1/Bi = 0$, and the curvature increases with $1/Bi$ as the convection is less proportionally reduced until the curves became very flat and all approach 1 as the inverse of the Biot number approaches infinity. For $Ra = 10$ in Fig. 6, the

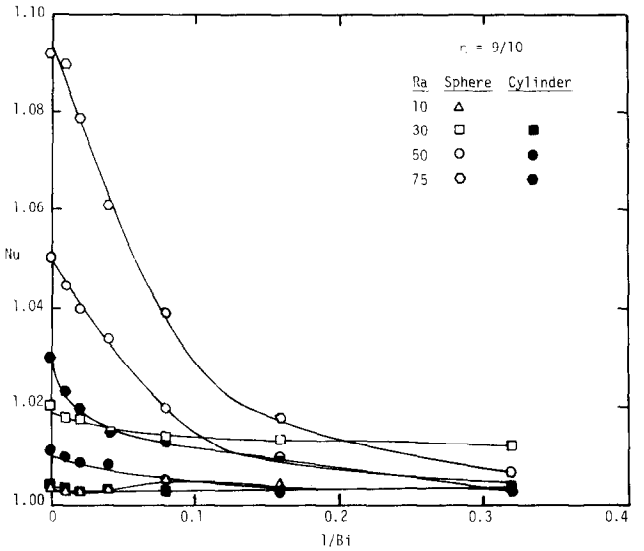

FIG. 6. The variation of the Nusselt number with the inverse of the Biot number for a radius ratio of $\frac{9}{10}$.

unexpected behavior is due to the inaccuracy of the results.

Streamlines and isotherms for $\eta = 1/2$ and Rayleigh numbers of 10 and 75 are shown in Figs. 7 and 8, respectively, for the spherical geometry. Streamlines are shown as solid lines, and isotherms are shown as dashed lines. An interesting aspect is the relatively stagnant portion in the lower region of the enclosure. Cold fluid flows into this region and assumes a relatively stable situation as there is little buoyancy force to impel the fluid to rise. The heat that would ordinarily flow radially by conduction is actually conducted very strongly azimuthally and subsequently carried away by the fluid as it turns upward near the lower portion of the inner boundary. Consequently, a relatively stagnant region exists in the lower portion of the sphere and a vigorous flow pattern exists in the upper portion of the sphere, especially near the line $\phi = \pi$. The center of the flow field, marked by an "X" on the drawings, shifts upward from the central location at $\phi = \pi/2$. With increasing Rayleigh number, the highly unstable condition existing near the top of the sphere might eventually manifest itself by tending towards longitudinal rolls, resulting initially in a separate "ring" vortex near the top of the enclosure. This

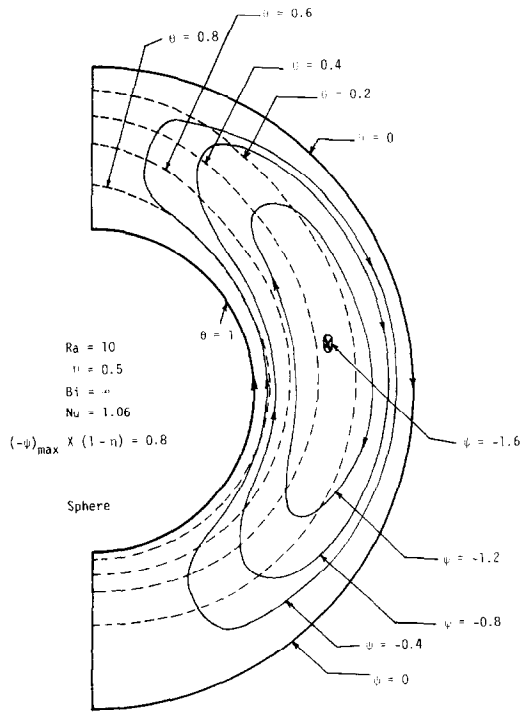

FIG. 7. Streamlines and isotherms for $Ra = 10$.

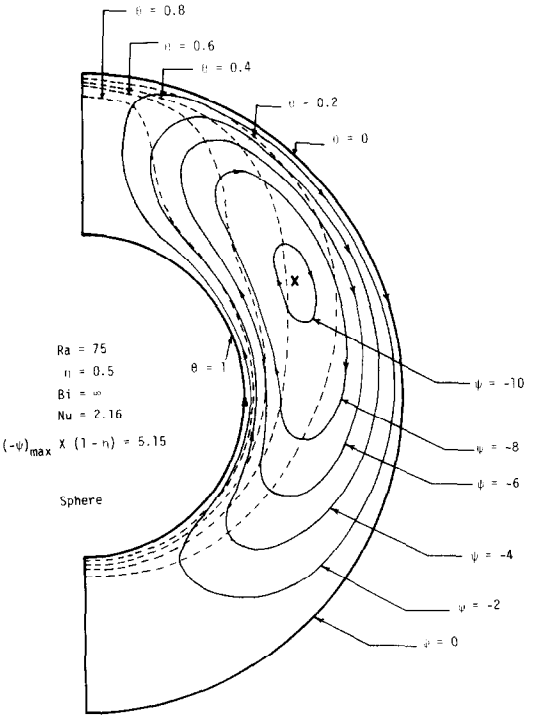

FIG. 8. Streamlines and isotherms for $Ra = 75$.

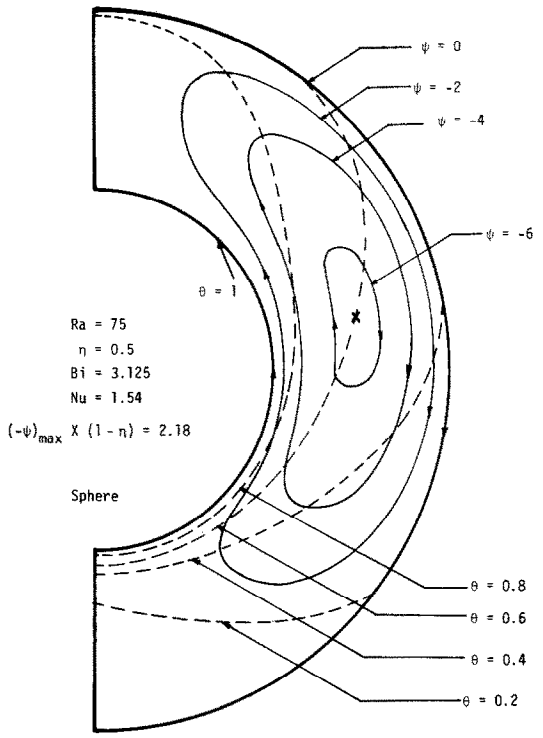

FIG. 9. Streamlines and isotherms for $Bi = 3.125$.

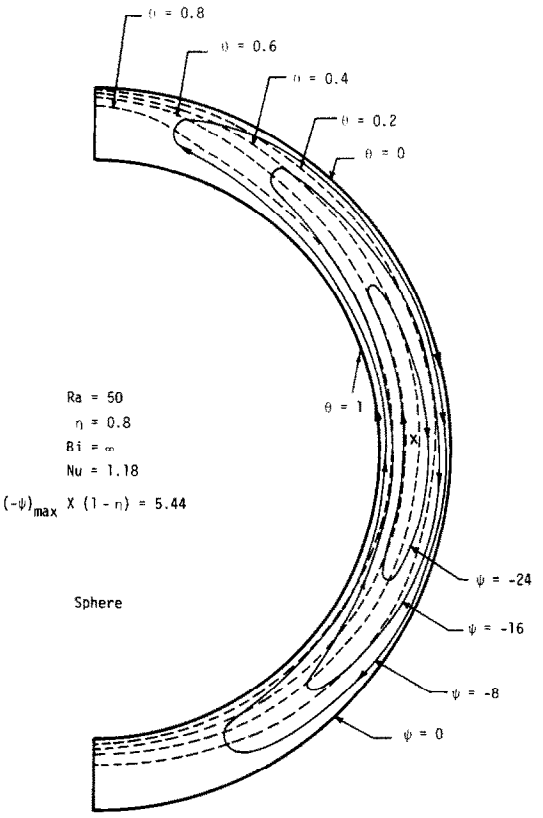

FIG. 10. Streamlines and isotherms for $\eta = 0.8$.

would be more probable for the higher radius ratios since they more closely resemble the flat plate "heated-from-below" geometry near $\phi = \pi$. The isotherms are seen to be distorted in accordance with the flow patterns.

The effect of the value of the Biot number upon the flow and temperature fields may be assessed by viewing the isotherms and streamlines for a Biot number of 3.125 in Fig. 9. At this radius ratio, the effect of Biot numbers greater than 50 are negligible as the field values are everywhere close to the infinite Biot number case. The net effect is that the entire outer boundary experiences an increase in temperature as evidenced by the horizontal spreading of the isotherms. The flow system is devitalized and the center of the flow decreases in angular position.

The effects of increasing the radius ratio may be evaluated by viewing Fig. 10, depicting streamlines and isotherms for $Ra = 50$, $Bi = \infty$ and $\eta = 0.8$. Although more vigorous, the flow contributes less significantly to the heat transport as the direction of flow occurs principally along lines of constant radial position. As before, the largest rates of heat transfer are seen to occur at the stagnation points existing at $\phi = 0$ and π for the inner and outer boundaries, respectively, with a gradual variation of the heat flux in the central portion.

For the cylindrical geometry at $\eta = 1/2$, the flow is slower and more uniform. The velocities near the walls are not as high, and the streamlines appear to follow the azimuthal grid lines more closely. The general flow pattern appears to be similar although the streamlines for the cylindrical geometry do not exhibit as pronounced an upward shift as do the streamlines for the spherical geometry. This is a manifestation of the lower overall rate of heat transfer for the cylindrical geometry at $\eta = 1/2$ as can be seen by comparing Figs. 2 and 3. The isotherms reflect this by appearing less distorted than for the spherical case.

PERTURBATION SOLUTION

In order to garner insight regarding the nature of the convection process concerning extrema and limits as the radius approaches zero, perturbation techniques were employed to solve equations (6) and (7). Only the results of the forms of the expressions for the spherical geometry will be reported herein, since the results for the cylindrical geometry are already available [16].

The stream function and the temperature are expanded in power series of the Rayleigh number as follows:

$$\psi = Ra^*\psi_1 + Ra^{*2}\psi_2 + Ra^{*3}\psi_3 + \ldots \quad (20)$$

$$\theta = \theta_0 + Ra^*\theta_1 + Ra^{*2}\theta_2 + \ldots \quad (21)$$

where Ra^* is the Rayleigh number dependent upon the outer radius, R_0. These expressions, when substituted into equations (6) and (7) and the boundary conditions, serve to essentially de-couple the perturbation functions when the limit of the Rayleigh number approaching zero is sequentially applied. The solutions are given in terms of a new radial coordinate $r' = \bar{r}/R_0$. The primes are dropped

and the solutions are as follows:

$$\theta_0 = \left(\frac{\eta}{1-\eta}\right)\left(\frac{1}{r} - 1\right) \tag{22}$$

$$\psi_1 = \left(\frac{\eta}{1-\eta}\right)\sin^2\phi\left(A_1 r^2 - \frac{r}{2} + \frac{A_2}{r}\right) \tag{23}$$

$$\theta_1 = \left(\frac{\eta}{1-\eta}\right)^2 \cos\phi\left(B_1 r + A_1 - \frac{1}{2r} + \frac{B_2}{r^2} - \frac{A_2}{r^3}\right) \tag{24}$$

$$\psi_2 = \left(\frac{\eta}{1-\eta}\right)^2 \sin^2\phi\cos\phi\left(A_3 r^3 - \frac{A^1}{4} r^2 + \frac{r}{6} - \frac{B_2}{2} + \frac{A_2}{r} + \frac{A_4}{r^2}\right) \tag{25}$$

$$\theta_2 = \left(\frac{\eta}{1-\eta}\right)^3\left[\left(B_3 r^2 + B_4 r + B_5 + \frac{B_6}{r} + \frac{B_7}{r^2} + \frac{B_8 + B_9 \ln r}{r^3} + \frac{B_{10}}{r^4} + \frac{B_{11}}{r^5}\right) + \cos 2\phi\left(B_{12} r^2 + B_{13} r + B_{14} + \frac{B_{15}}{r} + \frac{B_{16}}{r^2} + \frac{B_{17} + B_{18}\ln r}{r^3} + \frac{B_{19}}{r^4} + \frac{B_{20}}{r^5}\right)\right] \tag{26}$$

where the constants, A_i and B_i, are functions of the radius ratio, η, alone.

The first temperature modification does not contribute to the average heat flux due to the antisymmetric nature of the excess. This second correction to the temperature consists of a second harmonic proportion to $\cos 2\phi$ and a function of the new radial coordinate alone. Only the function dependent upon the new radial coordinate alone contributes to the average transfer of heat. The contribution to the average Nusselt number, defined by equation (10), is as follows:

$$Nu = 1 + Ra^2\left[\frac{-\eta^2}{(1-\eta)^4}(2B_3 + B_4 - B_6 - 2B_7 - 3B_8 + B_9 - 4B_{10} - 5B_{11})\right] + O(Ra^3). \tag{27}$$

For convenience, the function in the brackets will be called $g(\eta)$ as it is dependent upon the radius ratio alone. The Nusselt number may then be expressed to the order of Ra^2 as:

$$Nu = 1 + Ra^2 g(\eta) + O(Ra^3). \tag{28}$$

The perturbation analysis was carried no further as the algebra was becoming quite laborious. It is noted that the Rayleigh number here, Ra, is defined as before in equation (9).

The dependence of the convection contribution to the Nusselt number may be determined by viewing Fig. 11 which depicts the variation of $g(\eta)$ with η. The small dashed line is a representation of the curve fit, given by the formula: $0.0313[\eta(1-\eta)]^{1.9}\,e^{-3.62\eta}$. In contrast to the linear dependence upon the Rayleigh number of the heat transfer for the rectangular geometry [20], a quadratic dependence is observed here. The maximum occurs at $\eta = 0.3$. Further terms in the perturbation solution may yield higher order corrections which do not possess a maximum at this point.

The perturbation solution is seen to yield acceptable accuracy if the overall Nusselt number is below about $Nu = 1.6$. This yields the following range of validity:

$$Ra \leq \frac{0.775}{[g(\eta)]^{1/2}}. \tag{29}$$

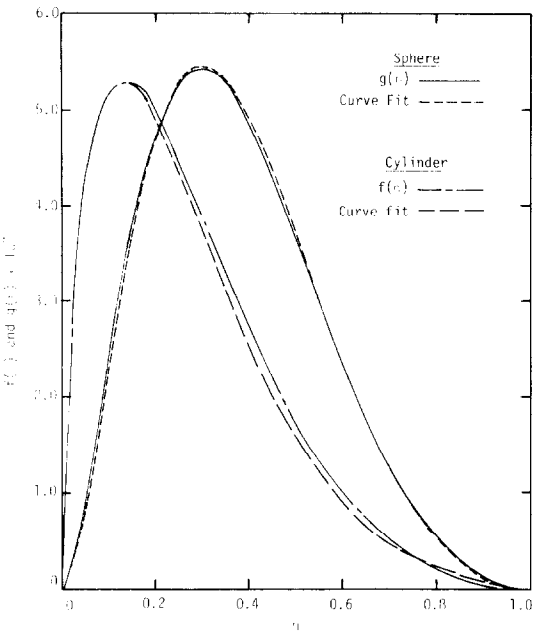

FIG. 11. Perturbation functions $f(\eta)$ ang $g(\eta)$.

Equation (28) is uniformly valid for all radius ratios below a Rayleigh number of about 35. As the radius ratio approaches zero and one the perturbation approximation grows progressively better with infinite radii of convergence for the Rayleigh number at the limiting radius ratios. The streamlines and isotherms calculated from equations (20) and (21) are in excellent agreement with the ones obtained from the numerical calculations for the above range of convergence and, consequently, will not be presented here.

A similar perturbation analysis for the cylindrical geometry yields:

$$Nu = 1 + Ra^2 f(\eta) + O(Ra^3). \tag{30}$$

The function $f(\eta)$, which contains the entire dependence of the Nusselt number on the radius ratio, is also shown in Fig. 11. The curve fit is represented by the large-dashed line:

$$5.9 \times 10^{-3}[\eta(1-\eta)]^{3/4}\,e^{-4.92\eta}.$$

A maximum is observed at a radius ratio of $\eta = 0.13$.

The results obtained from the perturbation analysis agree well with the results obtained from the

numerical calculations for Nusselt numbers below about $Nu = 1.4$, yielding the following range of validity:

$$Ra \leqslant \frac{0.632}{[f(\eta)]^{1/2}}. \quad (31)$$

COMPARISON WITH RESULTS OF FLUID-FILLED ENCLOSURES

The present results for the cylindrical geometry will be qualitatively compared with the results obtained by Kuehn and Goldstein [21] for the condition of a Newtonian fluid existing in the annular space. When no porous matrix is present, the conduction regime, in which the effect of convection upon the temperature field is negligible, occurs when $\overline{Ra} < 100$. Another flow regime is the boundary-layer regime occurring when the Rayleigh number is greater than about $\overline{Ra} = 3 \times 10^4$, and, for Rayleigh numbers between 100 and 3×10^4, a transition region exists. In the lower Rayleigh number region of the transition regime, the entire flow rotates about an elevated center. As the Rayleigh number is increased a constant vorticity core develops indicating "solid-body" rotation. A temperature inversion becomes apparent near $\overline{Ra} = 10^4$. As the Rayleigh number is increased still further into the boundary-layer region, a relatively stagnant core is observed with changes in the velocity and temperature occurring over a short distance, and the temperature inversions become severe. In this region, the Nusselt number is proportional to $\overline{Ra}^{1/4}$. The variation of the Nusselt number with the radius ratio is observed to undergo a maximum value near $\eta = 0.3$. The Prandtl number is seen to exert little effect throughout the investigation.

For the internal porous medium cases the conduction regime exists when the modified Rayleigh number is below about 1. In the present investigation, the nature of the flow field did not change as the modified Rayleigh number was increased to 75, although the distortion of the isotherms became more pronounced. A core region does not exist at any of the investigated Rayleigh numbers. Contrary to the Newtonian fluid results, the velocities are relatively high near the boundaries, resulting in much of the heat being convected away by the mass flowing adjacent to the boundary. The convection component of the Nusselt number is approximately proportional to the square of the modified Rayleigh number.

CONCLUSIONS

Free convective heat transfer between concentric cylinders and spheres has been analytically examined. The effects of the modified Rayleigh number, the radius ratio, and the external heat-transfer coefficient have been quantitatively analyzed. Natural convection has been shown to exert a significant effect upon the total heat transfer for modified Rayleigh numbers greater than about 10. Since no core region exists, ΔR is the pertinent length scale. The heat transfer by convection has been shown to be dependent upon the square of the modified Rayleigh number at small Rayleigh numbers. Maximum values of the effective thermal conductivity were observed for the spherical and cylindrical geometries at radius ratios of about 0.3 and 0.15, respectively. A gross upward shift of the flow field has been observed with an associated distortion of the isotherms. Perturbation analyses have demonstrated the dependence of the convective transport of heat upon the radius ratio and the Rayleigh number. Finally, a correspondence to the instance wherein the cylindrical annular region is filled solely with a Newtonian fluid has been examined with some similarity observed at smaller values of the Rayleigh number.

Acknowledgement—The authors gratefully acknowledge the aid of Dr. Frederick S. Sherman and the helpful comments of Dr. E. R. G. Eckert. This research was supported by the National Science Foundation through Grant NSF-ENG 75-19649.

REFERENCES

1. C. L. Tien and G. R. Cunnington, Cryogenic insulation heat transfer, *Adv. Heat Transfer* **9**, 349 (1973).
2. J. D. Verschoor and P. Greebler, Heat transfer by gas conduction and radiation in fibrous insulation, *Trans. Am. Soc. Mech. Engrs* **74**, 962 (1952).
3. J. R. Mumaw, Variations of the thermal conductivity coefficient for fibrous insulation materials, M.S. Thesis, The Ohio State University (1968).
4. E. L. Lopez, Techniques for improving the thermal performance of low-density fibrous insulation, *Prog. Aeronaut. Astronaut.* **23**, 153 (1969).
5. M. G. Kaganer, *Thermal Insulation in Cryogenic Engineering*, Translated from Russian by A. Moscona. Israel Program for Scientific Translations, Jerusalem (1969).
6. M. Muskat, *The Flow of Homogeneous Fluids Through Porous Media*. J. W. Edwards, Michigan (1946).
7. A. E. Scheidegger, *The Physics of Flow through Porous Media*. University of Toronto Press, Toronto (1974).
8. C. G. Bankvall, Natural convective heat transfer in insulated structures, Lund Inst. of Tech. Report 38 (1972).
9. C. G. Bankvall, Heat transfer in fibrous materials, *J. Testing Evaluation* **3**, 235 (1973).
10. D. Fournier and S. Klarsfeld, Some recent experimental data on glass fibre insulating materials and their use for a reliable design of insulations at low temperatures, ASTM STP 544, 223 (1974).
11. P. H. Holst and K. Aziz, A theoretical and experimental study of natural convection in a confined porous medium, *Can. J. Chem. Engng* **50**, 232 (1972).
12. S. A. Bories and M. A. Combarnous, Natural convection in a sloping porous layer, *J. Fluid Mech.* **57**, 63 (1973).
13. T. Kaneko, M. F. Mohtadi and K. Aziz, An experimental study of natural convection in inclined porous media, *Int. J. Heat Mass Transfer* **17**, 485 (1974).
14. B. K. C. Chan, C. M. Ivey and J. M. Barry, Natural convection in enclosed porous media with rectangular boundaries, *J. Heat Transfer* **92**, 21 (1970).
15. J. E. Weber, Convection in a porous medium with horizontal and vertical temperature gradients, *Int. J. Heat Mass Transfer* **17**, 241 (1974).
16. J. P. Caltagirone, Thermoconvective instabilities in a

porous medium bounded by two concentric horizontal cylinders, *J. Fluid Mech.* **76**, 337 (1976).
17. V. A. Brailovskaya, G. B. Pbtrazhitsky and V. I. Polezhaer, On the effect of convective heat exchange on thermal-insulating properties of permeable porous interlayers, presented at the 1977 International Seminar on Heat Transfer in Buildings, Dubrovnik, Yugoslavia. To appear in *Heat Transfer in Buildings*. Hemisphere.
18. G. S. Beavers and E. M. Sparrow, Non-Darcy flow through porous media, *J. Appl. Mech.* **26**, 711 (1969).
19. K. E. Torrance, Comparison of finite-difference computations of natural convection, *J. Res. Nat. Bur. Standards Math. Sci.* **72B**, 281 (1968).
20. P. J. Burns, L. C. Chow and C. L. Tien, Convection in a vertical slot filled with porous insulation, *Int. J. Heat Mass Transfer* **20**, 919 (1977).
21. T. H. Kuehn and R. J. Goldstein, An experimental and theoretical study of natural convection in the annulus between horizontal concentric cylinders, *J. Fluid Mech.* **74**, 695 (1976).

CONVECTION NATURELLE DANS LES MILIEUX POREUX LIMITES PAR DES SPHERES CONCENTRIQUES ET DES CYLINDRES HORIZONTAUX

Résumé—On présente les résultats d'une étude analytique de la convection naturelle dans des milieux poreux complètement enfermés entre des sphères concentriquès et des cylindres horizontaux. Le problème permanent et bidimensionnel est résolu par la méthode des différences finies et la méthode des perturbations régulières. On donne les variations du transfert thermique global en fonction du nombre de Rayleigh modifié, du coefficient de transfert externe adimensionnel et du rapport des rayons. Les résultats montrent qu'un maximum du transfert thermique se produit pour les géométries sphériques et cylindriques et dépend seulement du rapport des rayons. Les champs des vitesses sont comparés pour les deux géométries. Une configuration intéressante concerne une région froide relativement stagnante et stable à la base du volume si la surface interne est chauffée, ce qui déplace le centre de la circulation principale par rapport à l'horizontale. De plus on analyse une analogie entre la nature de la convection naturelle lorsque la cavité est emplie d'un milieu poreux ou d'un fluide newtonien seul. Des formules algébriques sont établies pour leur utilisation dans des applications pratiques.

NATÜRLICHE KONVEKTION IN PORÖSEN MEDIEN, BEGRENZT VON KONZENTRISCHEN KUGEL- UND HORIZONTALEN ZYLINDERFLÄCHEN

Zusammenfassung—Die vorliegende Arbeit berichtet über die Ergebnisse von analytischen Untersuchungen der natürlichen Konvektion in porösen Medien, die vollständig von konzentrischen Kugel- und horizontalen Zylinderflächen begrenzt sind. Das stationäre, zweidimensionale Problem wurde mit der Methode der finiten Differenzen und dem regulären Störungsansatz gelöst. Es wurden die Änderungen des Wärmedurchgangs mit der modifizierten Rayleigh–Zahl, mit dem dimensionslosen äuß eren Wärmeübergangskoeffizienten und mit dem Radienverhältnis abgeschätzt. Die Ergebnisse zeigen, daß ein Höchstwert der Wärmeübertragung für die kugelförmigen und zylindrischen Geometrien auftritt, der allein von dem Radienverhältnis für jede Geometrie abhängt. Das Strömungsfeld wurde untersucht und bei beiden Geometrien verglichen. Eine interessante Besonderheit ist das Auftreten einer relativ trägen und stabilen kalten Zone unten an der Ummantelung, wenn die innere umgebende Fläche beheizt wird. Dadurch wird das Zentrum der Hauptzirkulation aus der Horizontalen verschoben. Darüberhinaus wird eine mögliche qualitative Analogie zwischen den Arten der freien Konvektion für die Fälle untersucht, daß die Ummantelung einerseits mit einem porösen Medium und andererseits nur mit einem Newton'schen Fluid ausgefüllt ist. Abschließend werden einige algebraische Beziehungen der Daten für den praktischen Gebrauch angegeben.

ЕСТЕСТВЕННАЯ КОНВЕКЦИЯ В ПОРИСТЫХ СРЕДАХ, ОГРАНИЧЕННЫХ КОНЦЕНТРИЧЕСКИМИ СФЕРАМИ И ГОРИЗОНТАЛЬНЫМИ ЦИЛИНДРАМИ

Аннотация — В статье приведены результаты аналитического исследования естественной конвекции в пористых средах, заключенных между концентрическими сферами и горизонтальными цилиндрами. Стационарная двухмерная задача решалась методом конечных разностей и методом регулярных возмущений. Проведена оценка влияния на суммарный коэффициент переноса изменений модифицированного числа Релея, безразмерного значения внешнего коэффициента переноса тепла и отношения радиусов. Показано, что максимальное значение теплового

потока для сферических и цилиндрических конфигураций зависит исключительно от отношения радиусов. Проведено сравнение полей течения для обеих геометрий. Отмечен интересный факт наличия относительно заторможенной и устойчивой холодной области в нижней части замкнутого объёма при подводе тепла к внутренней ограничивающей поверхности, что смещает центр наиболее интенсивной циркуляции с горизонтального положения. Кроме того, рассмотрена возможная качественная аналогия между процессами свободной конвекции при заполнении объёма пористой средой или исключительно одной ньютоновской жидкостью. Наконец, предложен ряд обобщенных зависимостей для практических расчётов.